

Blood DNA methylation analysis reveals a distinctive epigenetic signature of vasospasm in aneurysmal subarachnoid hemorrhage.

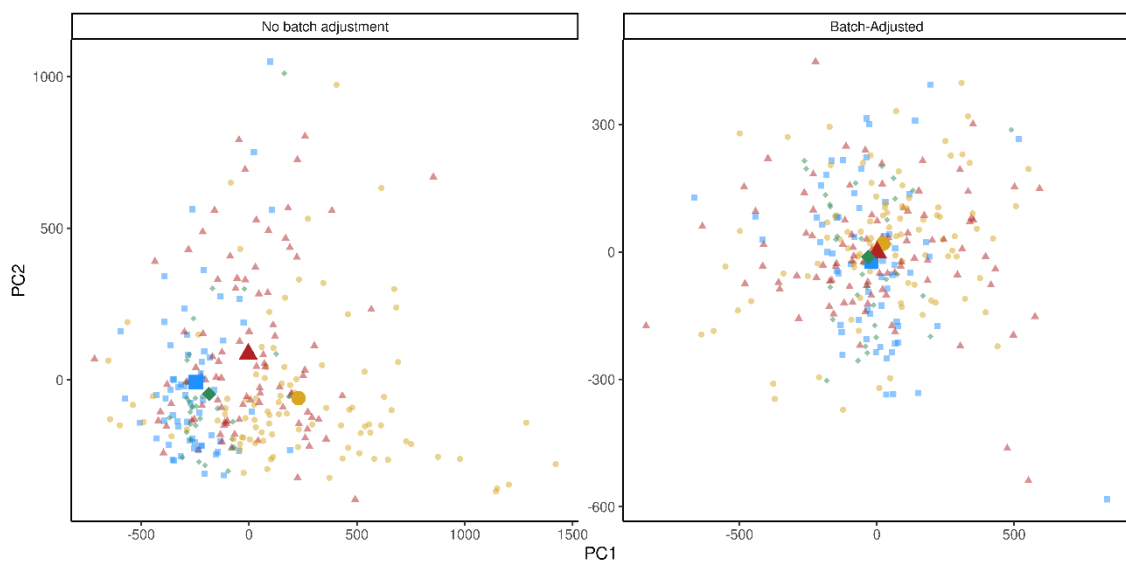
Isabel Fernández-Pérez, MD^{1,2}, Joan Jiménez-Balado, PhD², Adrià Macias-Gómez, MD^{1,2}, Antoni Suárez-Pérez, MD^{1,2}, Marta Vallverdú-Prats, PhD², Alberto Perez Giraldo, MD³, Marc Viles, MD⁴, Julia Peris, MD¹, Sergio Vidal, MD¹, Eva Giralt-Steinhauer, MD, PhD^{1,2,5}, Daniel Guisado-Alonso MD, PhD^{1,2}, Manel Esteller, MD, PhD^{6,7}, Ana Rodriguez-Campello, MD, PhD^{1,2,5}, Jordi Jiménez-Conde, MD, PhD^{1,2,5}, Angel Ois, MD, PhD^{*1,2,5}, Elisa Cuadrado-Godia, MD, PhD^{*1,2,5}

1. Neurology Department, Hospital del Mar, Barcelona, Catalunya, Spain
2. Neurovascular Research Group, Hospital del Mar Medical Research Institute, Barcelona, Catalunya, Spain
3. Neurosurgery Department, Hospital del Mar, Barcelona, Catalunya, Spain
4. Neuroradiology Department, Hospital del Mar, Barcelona, Catalunya, Spain
5. Pompeu Fabra University, Barcelona, Catalunya, Spain
6. Cancer Epigenetics Group, Research Institute Against Leukemia Josep Carreras, Badalona, Catalunya, Spain
7. Physiological Sciences Department, School of Medicine and Health Sciences, University of Barcelona, Barcelona, Catalunya, Spain

***contributed as last authors.**

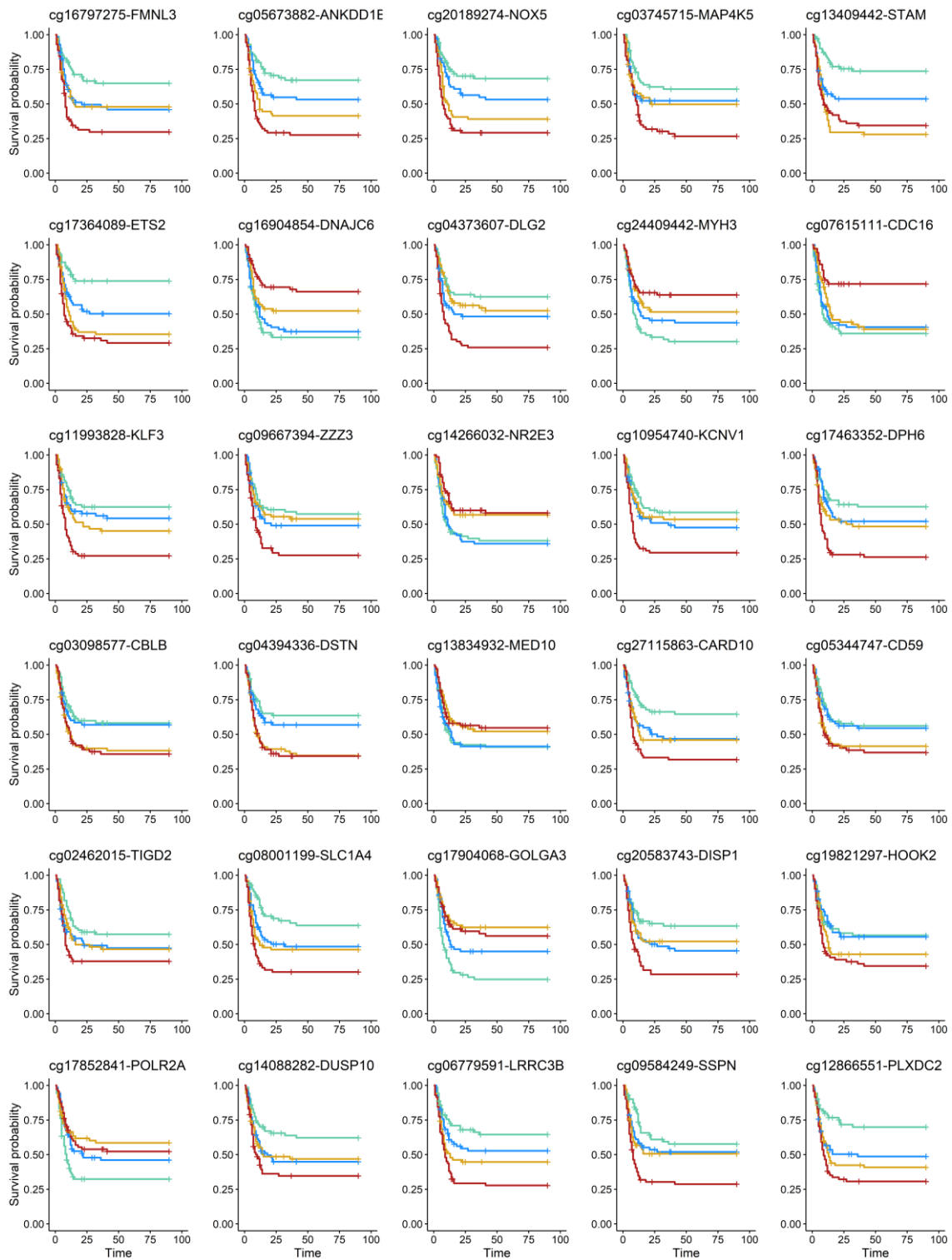
Corresponding author: Joan Jiménez Balado. E-mail address: jjimenez3@researchmar.net.

SUPPLEMENTARY FIGURES



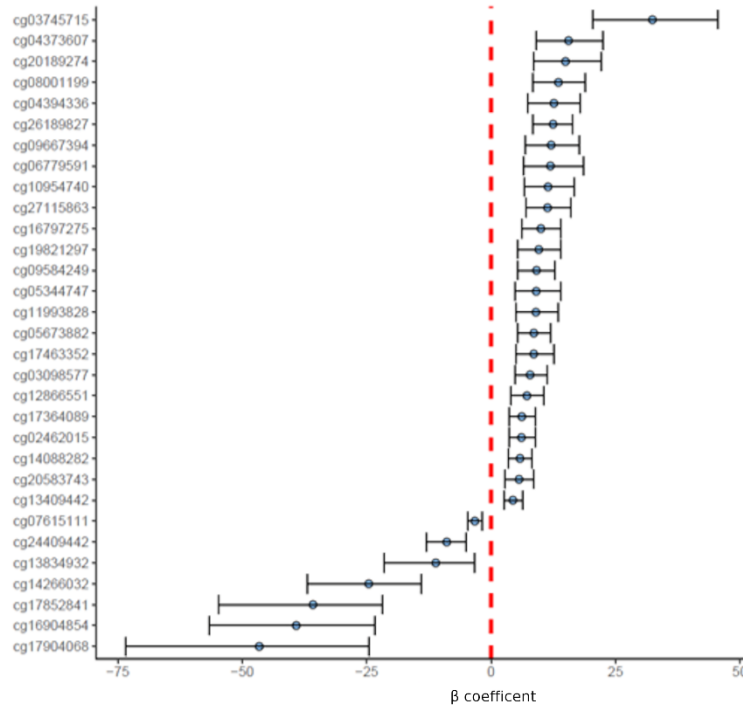
Supplementary figure 1: Adjustment for batch effect. We used principal components analysis to reduce the dimensions of DNAm dataset. In this plot we show the first dimension (PC1) against the second one (PC2) before (left panel) and after (right panel) adjusting for the batch effect. Each small dot represents a patient labeled (color and shape) according to the technical

run. Big dots represent the centroid of each technical run. As observed, batch adjustment reduced systematic differences between technical runs (centroids look closer).

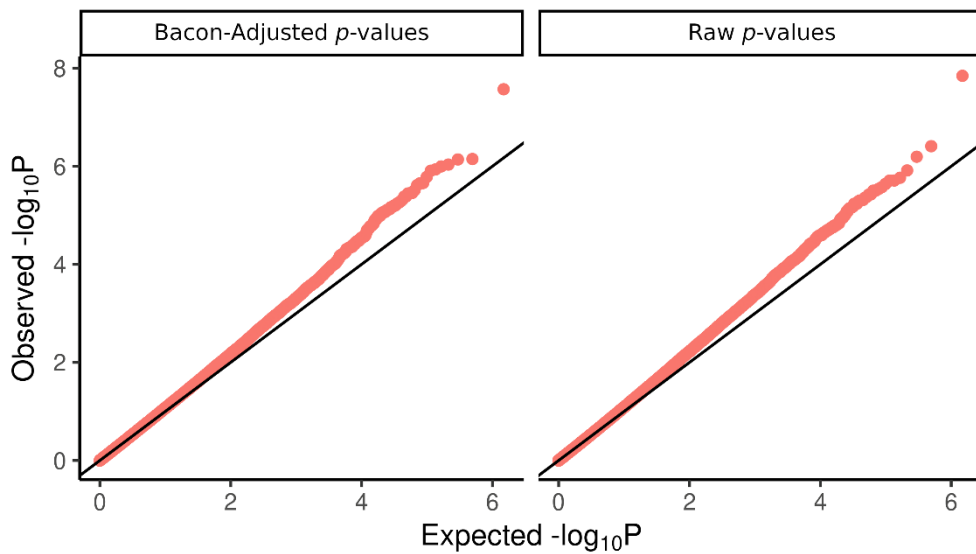


Supplementary figure 2: Effect of CpG candidates on incidence of vasospasm. In this figure we show the Kaplan-Meier curves of nominally significant DMPs (p -value $< 10^{-5}$). Labels at the top of each plot indicate the CpG labels (Illumina) and annotated gene (GREAT software). The X axis represents time in days, while the Y axis represents the survival function. Groups have

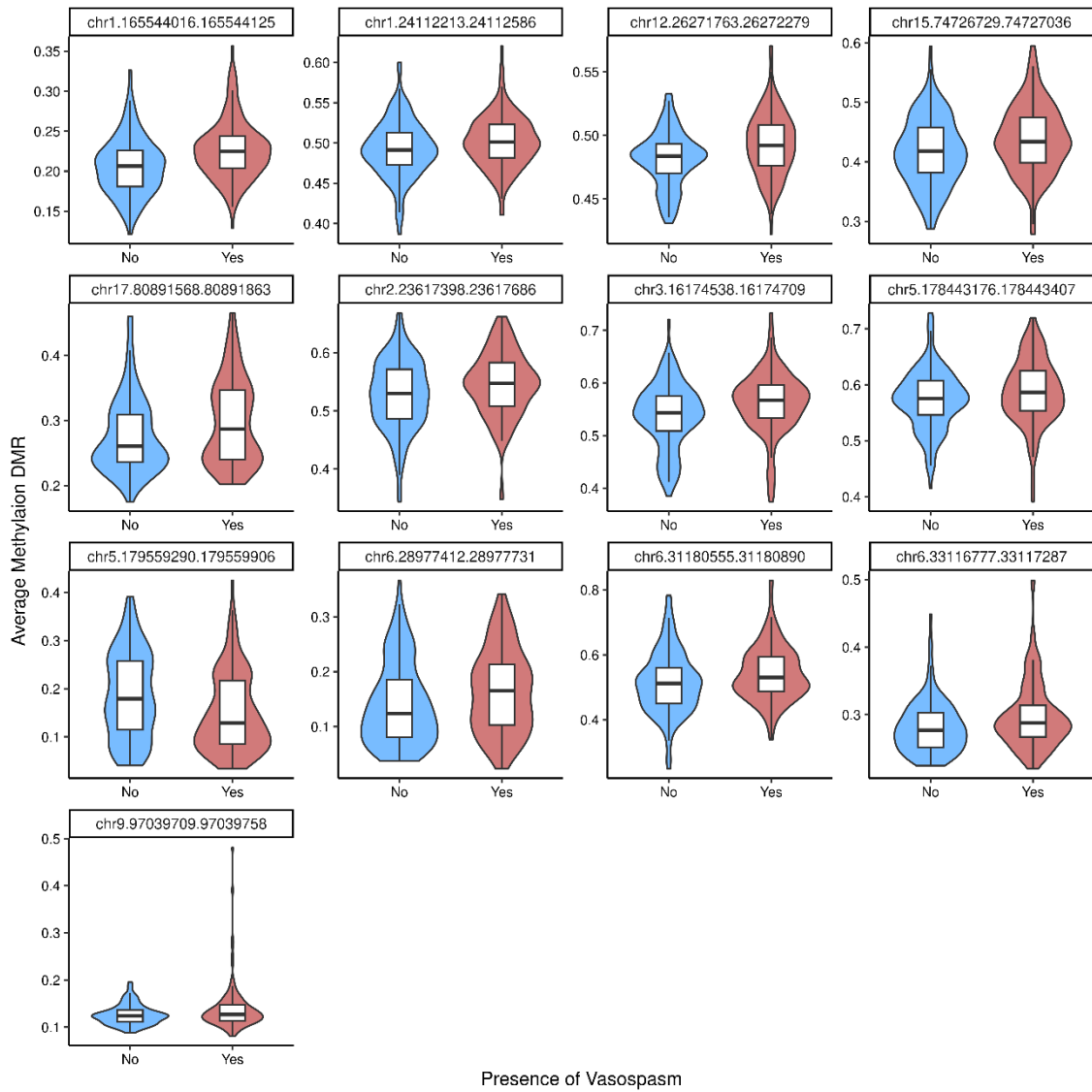
been obtained by discretizing methylation (β values) for each CpG according to quartiles distribution (light blue: first quartile; blue: second quartile; yellow: third quartile; red: fourth quartile).



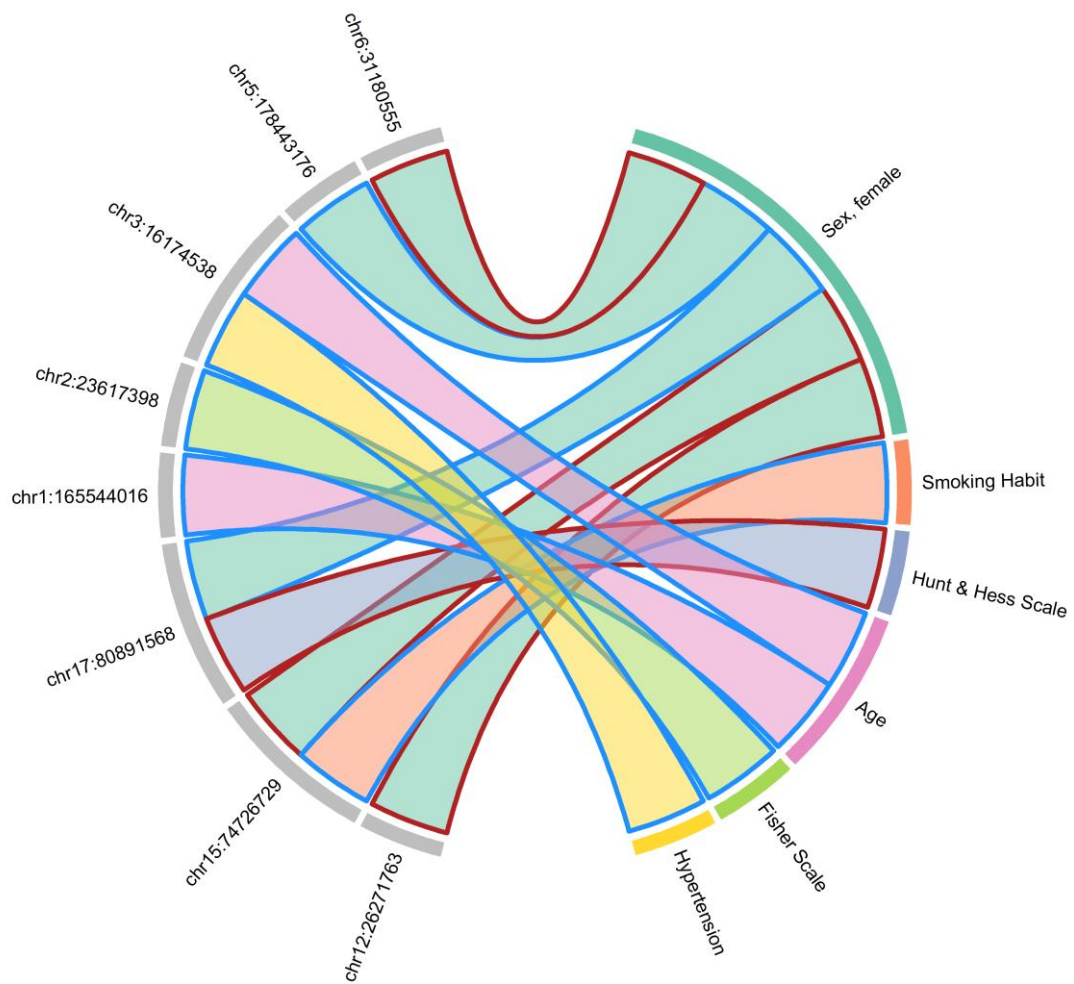
Supplementary figure 3: Bootstrap of significant DMPs found in the EWAS (table 2). We plotted the original β -coefficient of each CpG (dots) and the 99.9% confidence interval obtained after conducting the bootstrap (error bars). The vertical red dashed line corresponds to the absence of effect. Those CpGs crossing this line are not significant after doing the bootstrap, although no CpG was lost.



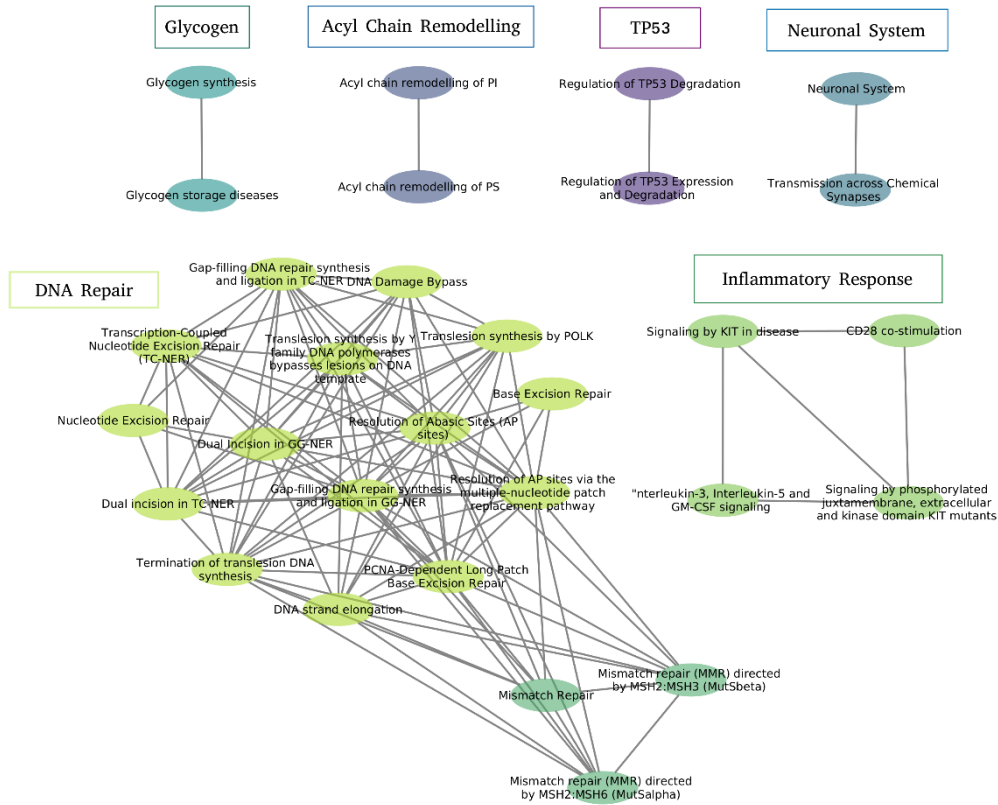
Supplementary figure 4: Adjustment for test-statistic inflation. Q-Q plot before and after doing test-statistic inflation adjustment (*Bacon*).



Supplementary figure 5: Average methylation at significant DMRs by presence of vasospasm. Violin plots comparing averaged methylation levels for each significant DMR between patients with and without vasospasm.



Supplementary figure 6: Relationship between average methylation of significant DMRs (left-side) and main risk factors and complications for vasospasm (right-side). DMRs are annotated according to the chromosome and the initial base-pair (table 3). In this figure we summarize significant relationships after adjusting for multiple testing (links). Border colors indicate a positive (red) or negative (blue) correlation. Filled colors represent distinct clinical factors.



Supplementary figure 7: Gene set enrichment analysis. We calculated the genes in common between all the possible combinations of significant pathways found in the gene set enrichment analysis (supplementary table 2). We then plotted the similarity of these sets as an acyclic graph. In this graph nodes represent pathways and edges that have been weighted according to the similarity coefficient (see the methods section). We filtered those nodes and edges having a similarity higher than 0.2. We finally clustered the graph using the autoannotate function (Cytoscape software). Each color represents an individual cluster.

SUPPLEMENTARY TABLES

Supplementary table 1

DNA methylation Quality Controls in the Sample	
Sample QCs (N=288)	
Sex mismatch	3
Call rate < 98%	0
Deviated median intensities	0
Final Sample size	285 (98.9%)
CpGs QCs (N=865918)	
1% samples detection p -value < .05	2940
Beadcount < 3 in 5% samples	3765
Non-CpG probes	2920
SNP positions	97039
Multi-hit CpGs	20
CpGs in X and Y chromosomes	16762
Final number of CpGs	742472

Supplementary table 1: In this table we summarize sample and CpG QCs. After applying all QCs, we kept 285 samples and 742,472 CpGs for the analyses.

Keywords: SNP, single-nucleotide polymorphism; QC, quality control.

Supplementary table 2

Gene set enrichment analysis of the epigenome-wide association study of vasospasm

Database ID	Description	Path size	Normalized enrichment score	p-value	Q value
Gene Ontologies database					
GO:0031941	Filamentous actin	30	1.41	2.29E-06	0.0188
GO:0032092	Positive regulation of protein binding	82	1.21	1.49E-05	0.0343
GO:0045773	Positive regulation of axon extension	38	1.34	1.75E-05	0.0343
GO:0030155	Regulation of cell adhesion	701	1.06	2.16E-05	0.0343
GO:0005244	Voltage-gated ion channel activity	189	1.12	3.00E-05	0.0343
GO:0022832	Voltage-gated channel activity	189	1.12	3.00E-05	0.0343
GO:0045785	Positive regulation of cell adhesion	414	1.08	3.00E-05	0.0343
GO:0048538	Thymus development	45	1.26	3.34E-05	0.0343
GO:0030010	Establishment of cell polarity	135	1.14	4.46E-05	0.0407
Reactome database					
R-HSA-110313	Translesion synthesis by Y family DNA polymerases bypasses lesions on DNA template	37	1.33	1.35E-05	0.0180
R-HSA-9725371	Nuclear events stimulated by ALK signaling in cancer	18	1.44	2.39E-05	0.0180
R-HSA-73933	Resolution of Abasic Sites (AP sites)	38	1.33	4.13E-05	0.0207
R-HSA-73893	DNA Damage Bypass	45	1.26	5.58E-05	0.0207
R-HSA-69190	DNA strand elongation	31	1.33	8.07E-05	0.0207
R-HSA-5696397	Gap-filling DNA repair synthesis and ligation in GG-NER	25	1.35	8.29E-05	0.0207
R-HSA-73884	Base Excision Repair	45	1.25	0.000106602	0.0207
R-HSA-5656169	Termination of translesion DNA synthesis	31	1.32	0.000112242	0.0207
R-HSA-5696400	Dual Incision in GG-NER	39	1.27	0.000123567	0.0207
R-HSA-71291	Metabolism of amino acids and derivatives	338	1.08	0.00016211	0.0240
R-HSA-6782135	Dual incision in TC-NER	63	1.20	0.000175713	0.0240
R-HSA-9669938	Signaling by KIT in disease	20	1.34	0.000303037	0.0340
R-HSA-9670439	Signaling by phosphorylated juxtamembrane, extracellular and kinase domain KIT mutants	20	1.34	0.000303037	0.0340
R-HSA-422475	Axon guidance	520	1.06	0.000316707	0.0340
R-HSA-6782210	Gap-filling DNA repair synthesis and ligation in TC-NER	62	1.20	0.000357719	0.0349

R-HSA-110373	Resolution of AP sites via the multiple-nucleotide patch replacement pathway	25	1.31	0.00037139	0.0349
R-HSA-389356	CD28 co-stimulation	32	1.27	0.000426072	0.0352
R-HSA-202433	Generation of second messenger molecules	29	1.28	0.000462527	0.0352
R-HSA-8943724	Regulation of PTEN gene transcription	59	1.19	0.000471686	0.0352
R-HSA-5696398	Nucleotide Excision Repair	107	1.13	0.000490003	0.0352
R-HSA-1482922	Acyl chain remodelling of PI	16	1.37	0.0005455	0.0352
R-HSA-5358508	Mismatch Repair	15	1.37	0.000554668	0.0352
R-HSA-112316	Neuronal System	387	1.06	0.00058159	0.0352
R-HSA-5655862	Translesion synthesis by POLK	17	1.37	0.000609676	0.0352
R-HSA-5358565	Mismatch repair (MMR) directed by MSH2:MSH6 (MutSalpha)	14	1.36	0.000618843	0.0352
R-HSA-5358606	Mismatch repair (MMR) directed by MSH2:MSH3 (MutSbeta)	14	1.36	0.000618843	0.0352
R-HSA-6804757	Regulation of TP53 Degradation	36	1.24	0.000645701	0.0352
R-HSA-6806003	Regulation of TP53 Expression and Degradation	37	1.24	0.00065486	0.0352
R-HSA-1474244	Extracellular matrix organization	292	1.07	0.000755606	0.0380
R-HSA-450604	KSRP (KHSRP) binds and destabilizes mRNA	17	1.36	0.00076553	0.0380
R-HSA-1170546	Prolactin receptor signaling	13	1.38	0.000783866	0.0380
R-HSA-3322077	Glycogen synthesis	15	1.35	0.000811369	0.0382
R-HSA-112315	Transmission across Chemical Synapses	255	1.07	0.001076885	0.0471
R-HSA-3229121	Glycogen storage diseases	14	1.35	0.001077962	0.0471
R-HSA-5651801	PCNA-Dependent Long Patch Base Excision Repair	21	1.29	0.001095293	0.0471
R-HSA-1482801	Acyl chain remodelling of PS	22	1.31	0.001168925	0.0477
R-HSA-6781827	Transcription-Coupled Nucleotide Excision Repair (TC-NER)	76	1.15	0.001187332	0.0477
R-HSA-512988	Interleukin-3, Interleukin-5 and GM-CSF signaling	45	1.19	0.00120574	0.0477
R-HSA-71387	Metabolism of carbohydrates	278	1.07	0.001242556	0.0479

Supplementary table 2. Using the EWAS summary statistics (table 2) we studied the gene-set enrichment for several databases: Gene-Ontologies, Reactome and KEGG. In this table we filtered those gene-sets with a Q-value < 0.05. For each gene-set (rows) we show the name, the number of annotated gene, the enrichment score, *p*-value and Q-value.